Effect of environmental and nutritional conditions on the formation of single and mixed-species biofilms and their efficiency in cadmium removal

Fathollahi, A. & Coupe, S.

Original citation:
Fathollahi, A & Coupe, S 2021, 'Effect of environmental and nutritional conditions on the formation of single and mixed-species biofilms and their efficiency in cadmium removal', Chemosphere, vol. 283, 131152.
https://dx.doi.org/10.1016/j.chemosphere.2021.131152

DOI 10.1016/j.chemosphere.2021.131152
ISSN 0045-6535

Publisher: Elsevier

Chemosphere 283 (2021) 131152

Contents lists available at ScienceDirect

Chemosphere

journal homepage: www.elsevier.com/locate/chemosphere

Effect of environmental and nutritional conditions on the formation of single and mixed-species biofilms and their efficiency in cadmium removal

Alireza Fathollahi *, Stephen J. Coupe

Centre for Agroecology Water and Resilience (CAWR), Coventry University, Wolston Lane, Ryton on Dunsmore, CV8 3LG, UK

ARTICLE INFO

Handling Editor: Dr A Adalberto Noyola

Keywords:
Actinomyces meyeri
Bacillus cereus
Escherichia coli
Pseudomonas fluorescens
Biofilm
Growth substrate
Biosorption
Cd(II) removal

ABSTRACT

Remediation of contaminated water and wastewater using biosorption methods has attracted significant attention in recent decades due to its efficiency, convenience and minimised environmental effects. Bacterial biosorbents are normally deployed as a non-living powder or suspension. Little is known about the mechanisms or rates of bacterial attachment to surfaces and effect of various conditions on the biofilm development, as well as efficiency of living biofilms in the removal of heavy metals. In the present study, the effect of environmental and nutritional conditions such as pH, temperature, concentrations of phosphate, glucose, amino acid, nitrate, calcium and magnesium, on planktonic and biofilm growth of single and mixed bacterial cultures, were measured. Actinomyces meyeri, Bacillus cereus, *Escherichia coli*, Pseudomonas fluorescens strains were evaluated to determine the optimum biofilm growth conditions. The Cd(II) biosorption efficiencies of the mixed-species biofilm developed in the optimum growth condition, were investigated and modelled using Langmuir, Freundlich and Dubnin Radushkevich models. The biofilm quantification techniques revealed that the optimum concentration of phosphate, glucose, amino acid, nitrate, calcium and magnesium for the biofilm development were 25, 10, 1, 1.5, 5 and 0.5 g L^{-1}, respectively. Further increases in the nutrient concentrations resulted in less biofilm growth. The optimum pH for the biofilm growth was 7 and alkaline or acidic conditions caused significant negative effects on the bacterial attachment and development. The optimum temperatures for the bacterial attachment to the surface were between 25 and 35 °C. The maximum Cd(II) biosorption efficiency (99%) and capacity (18.19 mg g^{-1}) of the mixed-species biofilm, occurred on day 35 (C_i = 0.1 mg L^{-1}) and 1 (C_i = 20 mg L^{-1}) of biofilm growth, respectively. Modelling of the biosorption data revealed that Cd(II) removal by the living biofilm was a physical process by a monolayer of biofilm. The results of present study suggested that environmental and nutritional conditions had a significant effect on bacterial biofilm formation and its efficiency in Cd (II) removal.

1. Introduction

Urbanization across the world has resulted in more impervious surface pavements, rooftops and parking lots (McGrane, 2016; Gwenzi and Nyamadzawo, 2014). Impervious surfaces have little or low infiltration capacity, in comparison with undeveloped space, which causes increased amounts of stormwater to be produced after heavy rainfall events (Walsh et al., 2012). Atmospheric deposition, accumulation on drainage surfaces and anthropogenic activities, such as industrial and construction activities, are reported to cause contamination of the urban stormwater as it runs off the impervious surfaces (Müller et al., 2020; Fathollahi and Coupe, 2021). Dissolved forms of heavy metals are mobilised by the stormwater and transferred to the receiving soil and water bodies (Wang et al., 2017). Contaminated urban runoff has been a concern to environmentalists in past decades, due to its significant contribution to deterioration of surface water quality and risk to water sources, such as rivers and groundwater (Bashir et al., 2020).

The European Union (EU) Water Framework Directive (Directive 2000/60/EC) published a list of priority pollutants found in stormwater including total suspended solid (TSS), metals and polycyclic aromatic hydrocarbons (PAH) (Directive 2013/39/EU) as well as guidelines to reduce the load of priority pollutants to the receiving catchments (Zgheib et al., 2012). Various studies have reported high concentrations of heavy metals in urban stormwater (Sakson et al., 2018; Gasperi et al., 2014; Becouze-Lareure et al., 2016; Selbig et al., 2012). Cadmium is a toxic heavy metal that can be accumulated in plants by active root

* Corresponding author.
E-mail address: ad2068@coventry.ac.uk (A. Fathollahi).

https://doi.org/10.1016/j.chemosphere.2021.131152
Received 22 February 2021; Received in revised form 29 April 2021; Accepted 5 June 2021
Available online 9 June 2021

uptake (Amari et al., 2017). Cadmium can eventually find its way to the food chain and human body and cause chronic and acute diseases (Jaishankar et al., 2014; Tchounwou et al., 2012). Moreover, studies have reported the negative effect of short-term and long-term exposure to cadmium for microorganisms (Doelman and Haanstra, 1984; McGrath, 1999; Megharaj et al., 2003).

Over decades, several methods have been introduced for the removal of heavy metals from contaminated runoff, including chemical methods such as precipitation, electrochemical treatment, oxidation/reduction and physical methods including ion exchange, reverse osmosis and filtration (Enaime et al., 2020; Pugazhenthiran et al., 2016). The biological method of heavy metal removal from contaminated water is also known as biosorption. Biosorption is a sorption technique in which the sorbent is a biological agent (Michalak et al., 2013). Some of the advantages of biosorption are the affordable production of the sorbent, limited negative effects for the environment, treatment of large volumes of contaminated water, effectiveness for multiple types of heavy metals and with wide ranges of pH and temperature. In biosorption there is no role for chemical agents and therefore lower volumes of toxic by-products (Ismail et al., 2014). Biosorbents are generally classified as the products of living organisms including bacteria, fungi, algae and yeast or non-living such as waste material from agriculture and industry (Adewuyi, 2020). Many studies have reported the efficiencies of various biosorbents in the removal of heavy metals from contaminated water (Martínez-Júarez et al., 2012; Rodríguez et al., 2012; Hassan et al., 2012; Kumar et al., 2012).

Microorganisms such as bacteria, algae and fungi have a natural tendency to attach to surfaces and produce extracellular polymeric substances (EPS). The surface attachment is followed by the development of biofilm structure that is ecologically superior to planktonic growth, in that biofilm organisms are protected from competitors and predators (Salgar-Chaparro et al., 2020). The EPS layer of bacterial, algal and fungal biofilms have functional groups that actively bind with metal ions (Gupta and Diwan, 2016; Decho and Gutierrez, 2017). Many studies have used dry powdered bacterial, algal and fungal biofilms for the remediation of contaminated water (Brinza et al., 2007; Sheikha et al., 2008; Ramsenthil et al., 2010; Mamisahebei et al., 2007). Recent studies have looked for the efficiencies of living bacterial biofilms in the removal of soluble metals (Fathollahi et al., 2020, 2021a).

Environmental and nutritional conditions are critical in the process of bacterial growth (Baquero and Negri, 1997; Stewart, 2003). Many studies have looked for the optimum condition for suspended bacteria (Uribe-Lorío et al., 2019; Šovljanski et al., 2020; Calicioglu et al., 2018). Few studies have addressed the effect of environmental and nutritional conditions on the attachment of bacteria to surfaces and biofilm development. Fathollahi et al. (2020) reported the efficiency of living biofilms grown on a non-woven geotextile sheet in the removal of soluble mercury within the structure of Sustainable Drainage Systems (SuDS) devices. SuDS devices are designed to manage large volumes of urban stormwater as quickly as possible and improve water quality (Charlesworth et al., 2003). However, no study has been conducted on the optimum conditions for developing living biofilms, to enhance their heavy metal removal efficiencies.

The present study was conducted to evaluate the growth patterns of single and mixed-species bacterial strains on a nonwoven propylene and polyethylene geotextile and to optimize the biofilm development conditions. The present study hypothesises that environmental conditions such as pH, temperature and concentrations of nutrients including phosphate and glucose have a significant influence on bacterial attachment to the surface of geotextile and subsequently development of a mature biofilm. The present study hypothesises that the optimized biofilm grown on geotextile has a high heavy metal biosorption capacity. In order to examine the hypothesis of the present study, the effect of pH, temperature and nutritional conditions on different bacterial species biofilm formation. In the next stage of the study, Cd(II) biosorption capacities and efficiencies of different stages of biofilm formation were evaluated and modelled to understand the nature of Cd(II) biosorption by the living bacterial biofilm. Moreover, the toxicity of different concentrations of Cd(II) on different species of bacteria and the role of biofilm in the protection of bacterial cells were evaluated. Cd(II) was selected for biosorption and toxicity studies due its significant presence in the urban runoff, its relatively complicated and expensive remediation techniques and its negative effects on environment, microorganisms and human health.

2. Materials and methods

2.1. Bacterial strains

Bacterial strains of Bacillus cereus DS16, Actinomyces meyeri CIP 13148, *Escherichia coli* O157:H7 and Pseudomonas fluorescens CP003194 were used, in the present study to evaluate their biofilm growth rate on geotextiles and their survival, in contact with different concentrations of Cd(II). All 4 bacterial strains in the present study were isolated from urban soils to simulate biofilms that naturally develop within SuDS devices (provided by ATCC, Virginia, US). A mixed culture of bacterial strains was used to find the optimum nutritional and environmental conditions for growth of the biofilm prior to its application in the biosorption of soluble Cd(II).

2.2. Geotextile and bioreactor

Biofilms were grown on a geotextile surface with a method described previously (Fathollahi et al., 2020, 2021b). This method relies on the ability of bacterial cells to adhere to the fabric of the geotextile and generate biofilm. A nonwoven propylene and polyethylene geotextile was used in this study as a surface for biofilm growth. The geotextile was a Terram product, widely used in Sustainable Drainage Systems (SuDS) as a filter/separator within the block paving sub-base construction (terram.com). This geotextile has a composition of 70% polypropylene and 30% polyethylene and is used to prevent the intermixing of aggregates in different layers of pavement construction.

Geotextile circles with a surface area of 65 cm^2 were washed, weighed (using a 5 decimal place Sartorius analytical scale) and labelled before applying to the reactor for biofilm development. The biofilm development reactor consisted of a plastic container (12L) with two air pumps secured at the bottom to keep aerobic condition for microorganisms within the bioreactor medium, providing and circulating the necessary oxygen. The dissolved oxygen (DO) was kept in range of 4–6 mg L^{-1} to maintain aerobic conditions.

2.3. Biofilm growth conditions

Single strains of B. cereus, A. meyeri, *E. coli*, P. fluorescens and a mixed culture of all four bacterial strains were grown using the method described by Vincent (1970), prior to their addition to bioreactor and biofilm growth. The bioreactor medium was supplemented with different concentrations of various nutrients such as sugars, salts and osmotic agents to evaluate their associated bacterial and biofilm growth. Geotextile circles were added to the medium and harvested after 1, 7, 14, 21, 28, 35 and 42 days depending on the intended assay.

2.3.1. Effect of nutrient type and concentration

To evaluate the nutrient type and concentration on the growth rate of bacterial strains and their associated biofilm formation, the bioreactor was supplemented with phosphate (0–50 g L^{-1}), glucose (0–40 g L^{-1}), amino acid (0–50 g L^{-1}), nitrate (0–3 g L^{-1}), calcium (0–10 g L^{-1}) and magnesium (0–10 g L^{-1}), prior to the addition of geotextile circles for biofilm formation. Geotextiles were incubated and harvested after 1, 7, 14, 21, 28, 35 and 42 days for bacterial and biofilm quantification assays.

2.3.2. Effect of environmental condition

Temperature and pH are two important environmental factors that affect the rate of bacterial and biofilm growth. In order to evaluate the impact of temperature and pH on growth rates of single and mixed strains of B. cereus, A. meyeri, *E. coli*, and P. fluorescens, the geotextile circles were placed in bioreactors with different temperatures of 15, 25, 35 and 45 °C prior to harvesting and biofilm quantification assays. Another set of geotextile circles were incubated in bioreactor at pH 4, 5, 6, 7, 8 and 9 to evaluate the growth of biofilm. Samples were taken from bioreactor medium to quantify the bacterial growth and compare with the biofilm development.

2.3.3. Effect of incubation time

The growth of bacterial biofilms also depends on the incubation time. In order to quantify the growth of single and mixed strains of B. cereus, A. meyeri, *E. coli*, P. fluorescens in different stages of biofilm development, geotextile circles were harvested after 1, 7, 14, 21, 28, 35 and 42 days of incubation. Samples were taken from bioreactor medium to quantify the suspended bacterial growth and compare this with the biofilm development.

2.4. Biofilm formation quantification assays

2.4.1. Colony Forming Units

The first approach in assessing biofilm growth was counting the viable bacterial cells on geotextile circles incubated in the bioreactor. Counting viable bacterial cells is known as a standard biofilm quantification method (Adentuji et al., 2012). To carry out this experiment, harvested geo-textile circles were agitated in 10 mL saline to remove the biofilm from the geotextile for plate counts. Saline was prepared by dissolving 5g sodium chloride in 1L deionized water and autoclaved for 15 min at 121 °C. A 1 mL sample from each geotextile circle was serially diluted prior to inoculation onto nutrient agar and incubated at 37 °C for 48 h, prior to counting viable cells, determined as Colony Forming Units (CFUs) per mL of sample. Nutrient agar had the following formula: yeast extract 2 g L^{-1}, peptone 5 g L^{-1}, sodium chloride 5 g L^{-1}, agar 15 g L^{-1} with a pH of 7.4 at 25 °C (provided by ThermoFisher Scientific).

2.4.2. Fourier Transform Infrared spectroscopy

The development of functional groups on bacterial biofilms were quantified by Fourier Transform Infrared (FTIR) spectroscopy. Biofilm samples from different assays were analysed by reflection FTIR with a cooled detector technique to analyse the absorption spectra of the bond in the range of 400–4000 cm^{-1}. The absorption ratio associated with different incubation times, nutrient and environmental conditions were used to quantify and compare the biofilm growth. A Nicolet iN10 Infrared Microscope (Thermo Fisher Scientific) was used in the present study for the FTIR quantification assays.

2.5. Cd(II) toxicity assay

Different concentrations of Cd(II) were applied to single and mixed strains of B. cereus, A. meyeri, *E. coli*, P. fluorescens to evaluate the maximum concentration of Cd(II) in which each strain could survive. Geotextile circles were harvested after 7, 14 and 21 days of incubation and 50 mL of different concentrations of Cd(II) were applied to them for 120 min at pH 7. After 120 min of contact time, samples were taken for counting viable cells according to section 2.4.1. The same assay was carried out for bacterial cultures taken from the bioreactor medium, to examine the role of geotextile and biofilm in protecting the bacterial cells. 50 mL of the suspended bacteria of different strains from bioreactors were also exposed to different concentration of Cd(II) ions to evaluate the maximum metal concentration each bacterial strain could survive in the suspension to compare with the results from biofilms developed on geotextiles. After 120 min of contact time, samples were taken for serial dilution and nutrient agar plate counts (section 2.4.1).

2.6. Batch biosorption experiments

The efficiency of biofilms grown on geotextile fibres in removal of soluble Cd(II) ions was carried out by harvesting geotextile circles after 21 days of incubation. 10 mL of different concentrations of 0.1, 0.2, 0.5, 1, 2, 5, 10 and 20 mg L^{-1} Cd(II) solution were applied to geotextile circles for 120 min at pH 5.5 and 25 °C to evaluate the effect of initial concentrations of Cd(II) on the biosorption efficiency. 1 M NaOH solution was used to adjust the pH of the Cd(II) solutions. After 120 min, the solution was filtered through geotextile and samples were taken for quantification of Cd(II) concentration to calculate the biosorption efficiencies. A Perkin-Elmer optima 5300 DV ICP-OES instrument was used for the analysis to measure the equilibrium concentration of Cd(II) in filtered solution. The removal efficiencies of the mixed culture bacterial biofilm were quantified using the equation below:

$$R = \frac{(C_i - C_e)}{C_i} \times 100$$

where R is Cd (II) removal efficiency (%), C_i is initial concentration of the metal solution (mg L^{-1}) and C_e is the concentration of Cd(II) ions in the solution at biosorption equilibrium state (mg L^{-1}). Moreover, the biosorption capacities per gram of the 21 days incubated biofilm for different concentrations of soluble Cd(II) ions was calculated as follows:

$$q_e = \frac{(C_i - C_e)}{m} \times V$$

where q_e is the amount adsorbed Cd(II) ions on biofilm surface (mg g^{-1}), m is the mass of biosorbent (g) and V is the volume of the stock Cd (II) solution (L).

2.6.1. Control experiments

To evaluate the ability of geotextile fibres in the removal of Cd(II) ions and its possible interference in the biofilm removal efficiencies, a set of clean and sterilized geotextile circles were added to a bioreactor with the same nutrient and environmental conditions as original batch biosorption assays, with no bacterial strains added. This approach simulated the same conditions, representing minimal growth of biofilm. Geotextile circles were harvested after 21 days and the batch biosorption assay described in section 2.6 was carried out. Samples were taken for ICP-OES analysis to evaluate the Cd(II) removal efficiency of the clean geotextile fibres.

2.7. Chemicals and reagents

Analytical grade NaOH (Sigma Aldrich, 98% purity) was used to prepare 1 M sodium hydroxide solution for adjustment of pH in all assays. An analytical grade 1000 mg L^{-1} stock Cd(II) solution (provided by Perkin Elmer) was used for preparation of different cadmium concentrations in toxicity and biosorption assays. The nutrient agar used for CFU plate count assays was provided by ThermoFisher Scientific. The following sources were used as nutrients: Glycine ($C_2H_5NO_2$; as amino acid), sodium phosphate monobasic monohydrate ($NaH_2PO_4{\cdot}H_2O$; as source of phosphate), sodium nitrate ($NaNO_3$; as source of nitrate), magnesium chloride ($MgCl_2$; as source of magnesium) and calcium chloride ($CaCl_2$; as source of calcium), all purchased in analytical grade from Sigma Aldrich.

2.8. Statistical analysis

All the assays in the present study were carried out using 5 replicates. The statistical analysis was performed using SPSS software (Version 21.0, SPSS, Chicago, Illinois). In all biofilm formation quantification and batch biosorption assays a p-value less than 0.05 was considered to be statistically significant.

3. Results and discussion

3.1. Biofilm growth pattern

Fig. 1a presents the CFUs growth pattern of B. cereus, A. meyeri, *E. coli*, P. fluorescens and a mixed culture of all 4 strains on day 1, 7, 14, 21, 28, 35 and 42 of incubation, as an indicator of biofilm growth on the geotextile. The developed biofilms on the geotextile circles were detached into 10 mL of deionized water, prior to spread plate quantification of the biofilm growth. According to the results, A. meyeri strain was able to produce a biofilm with a maximum viable cell density of 8.2×10^9 CFU mL^{-1} occurring on day 21 of the biofilm growth. CFU associated with A. meyeri strain had a 0.7-log reduction between day 28 and 35 with 0.6-log increase on day 42. The 1-day incubated biofilm developed by the B. cereus strain contained 4.9×10^4 viable cells and showed a continuous logarithmic growth with the maximum occurring on day 28 of the incubation (2.1×10^{10} CFU mL^{-1}). This trend changed between day 28 and 35 with a 0.8-log reduction in the number of viable cells followed by an increase in viable cells on day 42. *E. coli* strain showed a rapid development of the biofilm with the maximum viable cells appearing on day 14 of incubation (4.3×10^9 CFU mL^{-1}) after which a 1-log decrease in the number of cells was observed. However, this decrease was completely recovered between day 28–35 followed by another decrease occurring on day 42. The biofilm developed by P. fluorescens strain contained 4×10^3 CFU mL^{-1} after one day of incubation with a rapid and continuous increase until day 21 (9.2×10^8 CFU mL^{-1}). However, the decrease of viable cells was observed from day 21–28 followed by an increase on day 35.

By comparing the number of viable cells within the biofilms, developed on the geotextile circles by all 4 bacterial strains, in the present study following results were obtained:

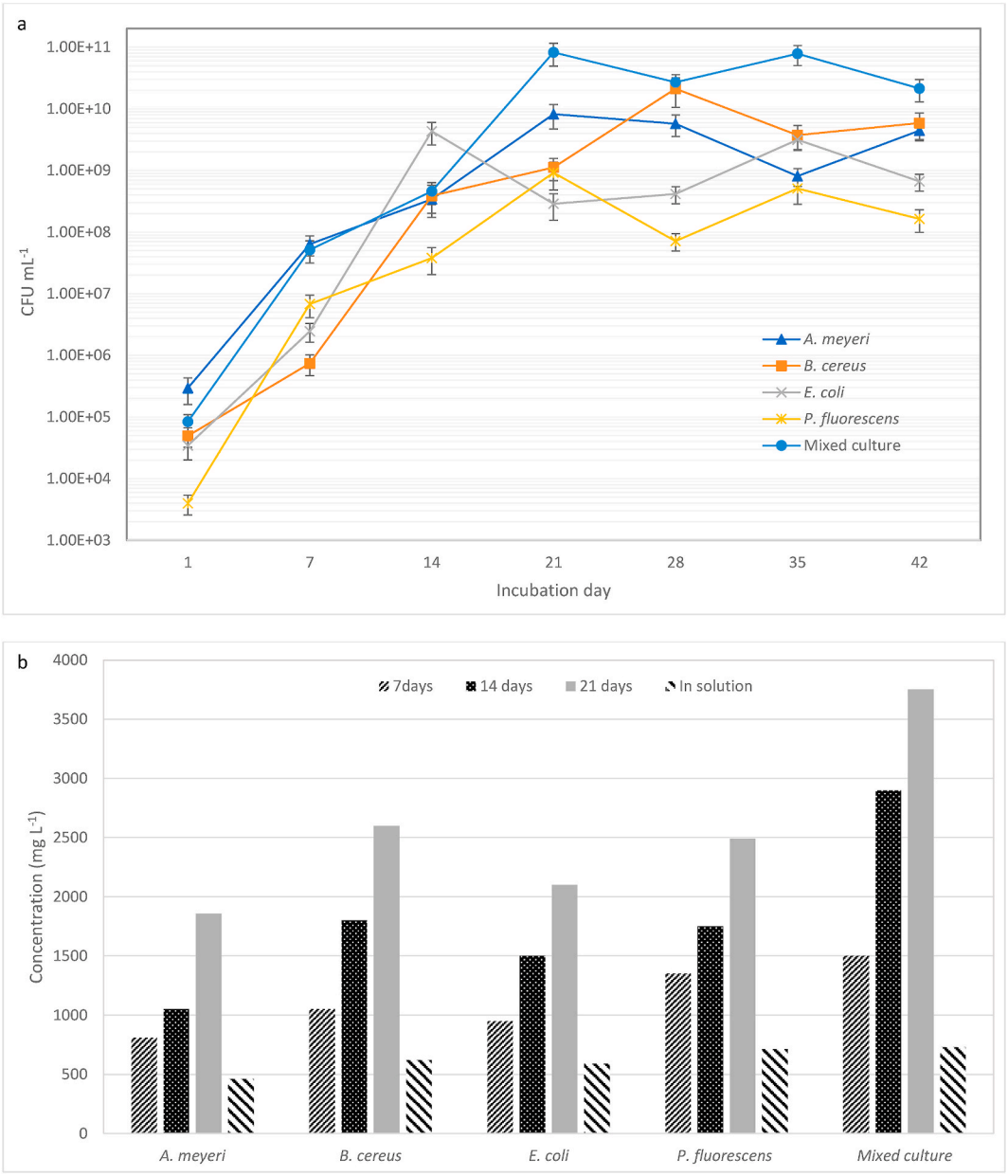

Fig. 1. a) Viable cells of single and mixed-species bacteria on different days of biofilm incubation. Data are expressed as mean ± standard deviation ($p < 0.05$). b) Toxicity of different concentrations of Cd(II) for bacterial species on biofilm and in bioreactor solution at pH 7, 25 °C and 120 min contact time. Reported numbers are the maximum concentrations of Cd(II) in which bacterial cells survived.

- Maximum viable cells were associated with the biofilm developed by B. cereus (2.1×10^{10} CFU mL^{-1}).
- The mature biofilm grown by A. meyeri, B. cereus, *E. coli* and P. fluorescens contained a maximum of 8.2×10^{9}, 2.1×10^{10}, 4.3×10^{9} and 9.2×10^{8} CFU mL^{-1}, respectively.
- *E. coli* was the fastest to reach the maximum possible viable cells within the biofilm (day 14).
- A. meyeri and P. fluorescens strains reached the maximum CFU mL^{-1} on day 21.
- B. cereus was the slowest to reach the maximum viable cells on day 28 of incubation.

- All 4 strains of bacteria showed a rapid increase in viable cells in the first 14 days of the biofilm development and from day 21–45 of incubation a periodic reduction and increase of cells were observed.

As described above, all 4 strains of bacteria showed a cycle of reduction and increase of viable cells starting from day 14, 21 or 28 of incubation. This observation was consistent with the nature of biofilm growth stages. Bacterial biofilm formation and maturation starts with the introduction of bacteria to a surface during a process originated by Brownian, gravitational and hydrodynamic forces (Beloin et al., 2008). Environmental factors such as pH and temperature as well as nutrient levels are reported to be influential on the strength of forces involved in adherence of bacteria on surfaces (Donlan, 2002). The effects of these factors on the biofilm growth have been evaluated in the present study and will be discussed in section 3.4. The next stage after the adherence of the bacteria to the surface is the formation of extracellular polymeric substance (EPS) and maturation of the biofilm (Di Martino, 2018). Harmston et al. (2010) have reported the important role of environmental conditions such as pH and temperature on the composition of extracellular matrix. In the third stage of biofilm growth the dispersion mechanisms start. Biofilm is a community of microorganisms that can actively change the structure of the biofilm and maintain the living environment (Kostakiot et al., 2013). During the dispersion stage of the biofilm growth, some mature parts of EPS are detached from the structure and the cells within the part are released to the medium, in a process known as sloughing (Kaplan, 2010). The dispersed microorganisms start another cycle of biofilm formation and adhere to a new surface to continue maturation and development a new biofilm layer (Gulati and Nobile, 2016). The results from the present study and the continuous increase and reduction of viable cells within the structure of biofilms developed by B. cereus, A. meyeri, *E. coli*, P. fluorescens strains can be explained by the cycling between the maturation and dispersion stages of the biofilm growth. According to Fig. 1a, the dispersion stage of the biofilm associated with B. cereus, A. meyeri, *E. coli*, P. fluorescens starts on day 28, 21, 14 and 21, respectively. Moreover, the duration of a cycle of maturation and dispersion of biofilm was 14 days for P. fluorescens and B. cereus strains. However, A. meyeri and *E. coli* strains showed a longer cycle of dispersion and maturation stages (21 days).

According to Fig. 1a the biofilm associated with the mixed culture of 4 bacterial strains reached the highest number of viable cells (8.3×10^{10} CFU mL^{-1}) which was 1-, 0.6-, 1.4- and 1.9-log higher than the maximum cells within the biofilm produced by A. meyeri, B. cereus, *E. coli*, P. fluorescens strains respectively. This finding was consistent with previous studies (Fan et al., 2020; Elias and Banin, 2012). The mixed species biofilm showed a rapid 6-log increase of viable cells from day 1 to day 21 where the maturation of biofilm was completed, and the dispersion stage started. The second cycle of dispersion occurred on day 35, which revealed the 14-day duration of maturation-dispersion cycle of the mixed species biofilm.

3.2. Toxicity of Cd(II) for bacterial species and biofilms

In the toxicity assay, geotextile circles were harvested on day 7, 14 and 21 of the biofilm incubations prior to application of 50 mL of different concentrations of Cd(II) ions for a duration of 120 min at pH 7. Day 7, 14 and 21 were selected to represent different stages of biofilm growth including attachment, maturation and dispersion phases. 50 mL of the suspended bacteria of A. meyeri, B. cereus, *E. coli*, P. fluorescens strains from bioreactors were exposed to different concentration of Cd (II) ions for a duration of 120 min at pH 7, to evaluate the maximum metal concentration each bacterial strain could survive in the suspension, as well as within the structure of biofilm. The results of maximum concentration of Cd(II) ions in which single and mixed species of A. meyeri, B. cereus, *E. coli*, P. fluorescens strains could survive in a suspension and as a biofilm, are presented in Fig. 1b.

Suspended strains of A. meyeri survived to a maximum concentration of 460 mg L^{-1}. However, a 7-day incubated biofilm of the same species provided protection to a maximum of 810 mg L^{-1}. The protection of the biofilm increased by maturation of that biofilm and the maximum tolerance of the A. meyeri against Cd(II) ions, increased to 1050 and 1857 mg L^{-1} on day 14 and 21 of incubation, respectively. This observation is consistent with previous studies which indicated that the EPS layer of bacterial biofilms can provide protection against severe environmental condition such as low pH, high temperature and heavy metal concentrations (Yin et al., 2019; Abebe, 2020; Karygianni et al., 2020). The establishment of the biofilm influences the cells through a passive process and alters the pattern of gene expression which results in tolerance against heavy metal concentrations as was observed in the present study (Araújo and de Oliveira, 2019; Koechler et al., 2015). Moreover, the organic structure of the biofilm acts as a barrier that isolates the bacterial cells from outer environmental condition such as heavy metals toxicities (Koechler et al., 2015). The same pattern of protection by 7-, 14- and 21-days incubated biofilms were observed for B. cereus, *E. coli*, P. fluorescens strains. The 21-days incubated biofilm increased the Cd(II) tolerance of *E. coli* from 590 mg L^{-1} in the suspension to 2150 mg L^{-1}. The maximum single species Cd(II) resistance in suspension was associated with P. fluorescens (710 mgL^{-1}) and the lowest Cd(II) tolerant species was A. meyeri (460 mg L^{-1}). Moreover, the maximum observed tolerance against Cd(II) ions within a 7-, 14- and 21-days incubated biofilm, were from P. fluorescens with 1340, 1760 and 2450 mg L^{-1}, respectively.

As shown in Fig. 1b, the mixed species bacterial biofilm showed tolerance against 1550, 2950 and 3750 mg L^{-1} of Cd(II) on day 7, 14 and 21 of biofilm growth, respectively. This observation revealed 11, 65 and 54% higher tolerance against Cd(II) ions on day 7, 14 and 21 of incubation in comparison with the most Cd(II) tolerant singles species biofilm in the present study (P. fluorescens). This may be a result of metabolic interactions between different species of the bacteria within the mixed-species biofilm which allowed the bacterial cells to be more tolerant against harsh conditions and as a result higher survival rates in comparison with single species biofilms (Elias and Banin, 2012). Moreover, the higher density of cells in the mixed-species biofilm that was observed in Fig. 1a, may have promoted the horizontal gene transfer process which resulted in higher tolerance against Cd(II) toxicity (Saini et al., 2011).

3.3. Effect of type and amount of nutrient on biofilm formation

The type and amount of nutrients in the bioreactor medium has a significant effect on the formation of bacterial biofilms (Haney et al., 2018; Salgar-Chaparro et al., 2020). In order to evaluate the effect of type and amount of nutrients on the formation of biofilm on the geotextile in the present study, a mixed-species culture of A. meyeri, B. cereus, *E. coli*, P. fluorescens strains were inoculated into bioreactors with different amount of nutrients including: phosphate (0–50 g L^{-1}), glucose (0–40 g L^{-1}), amino acid (0–50 g L^{-1}), nitrate (0–3 g L^{-1}), calcium (0–10 g L^{-1}) and magnesium (0–10 g L^{-1}).

The quantification of biofilm growth was carried out using 3 assays:

1. Harvesting the geotextile circles from the bioreactor and performing the plate count assay to count the viable cells (Fig. 2).

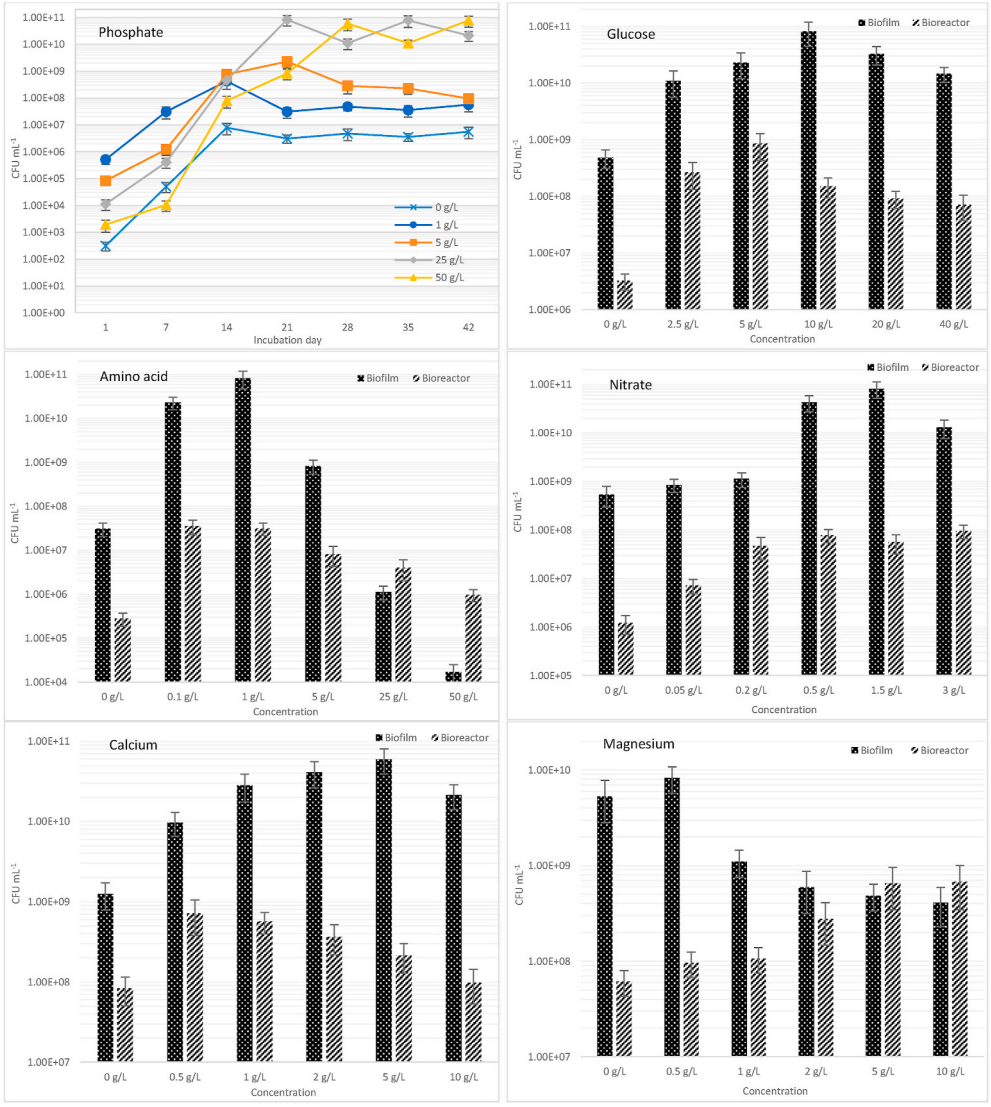

Fig. 2. Effect of concentration of different nutritions on number of viable cells on day 21 of mixed-species bacterial planktonic and biofilm growth. Data are expressed as mean ± standard deviation ($p < 0.05$).

2. Drying the harvested geotextile circles in different stages of biofilm growth prior to drying in oven at 65 °C for 72 h and weighing to record the dried biofilm mass (Fig. 3).
3. Performing FTIR microscopy analysis on the grown biofilm in different nutrient conditions to measure and compare the absorbance ratios (Fig. 4).

3.3.1. Phosphate

As shown in Fig. 2, the maximum viable cell density on the mixed-species biofilms were recorded for 25 g L^{-1} of phosphate in the bioreactor medium (8.2×10^{10} CFU mL^{-1}). The results from mass analysis of the biofilm growth (Fig. 3) confirmed this observation with the maximum mass of biofilm on day 21 of incubation, occurring at 25 g L^{-1} of phosphate. In general, with the increase of phosphate content in the bioreactor, the growth of the biofilm increased. At 50 g L^{-1} of phosphate content this trend reversed where viable cells and mass of the biofilm decreased. This observation may be due to the osmotic conditions caused by the hypertonic environment which initiates the shrinkage of bacterial cells (Brocker et al., 2012). The FTIR analysis of the generated biofilms confirmed that the 25 g L^{-1} of phosphate content was the optimum concentration for the mixed-species biofilm growth. According to Fig. 4, the maximum absorbance ratio was recorded on day 21 of the biofilm growth with 25 g L^{-1} of phosphate content. Moreover, the results of the viable cell count (Fig. 2) revealed that biofilms incubated in lower concentrations of phosphate (1 g L^{-1}) reached a lower maximum of growth in a shorter time (day 14). The lower maximum growth was due to a lack of nutrition content and as a result lower numbers of viable cells (Reezal et al., 1998; Bibby and Urban, 2004). The FTIR (Fig. 4) and mass analysis (Fig. 3) of the biofilm also revealed the lower absorbance ratio and mass of the biofilm with 1 g L^{-1} content of phosphate.

3.3.2. Glucose

The results from 3 quantification assays evaluating the effect of glucose content in the bioreactor on the growth of mixed-species biofilm, are presented in Figs. 2–4. According to Fig. 2, the maximum viable cells were observed at 10 g L^{-1} content of glucose (8.65×10^{10} CFU mL^{-1}). By increasing the glucose content to 20 and 40 g L^{-1} the number of bacterial cells within the biofilm decreased by 0.5- and 0.7-log, respectively. However, the suspended mixed-species bacteria in the bioreactor, showed maximum growth at 5 g L^{-1} of glucose content. The number of viable cells decreased by 1-log with further increase in the amount of glucose content. This observation was because biofilm growth has a threshold in the amount of utilisable glucose (Waldrop et al.,

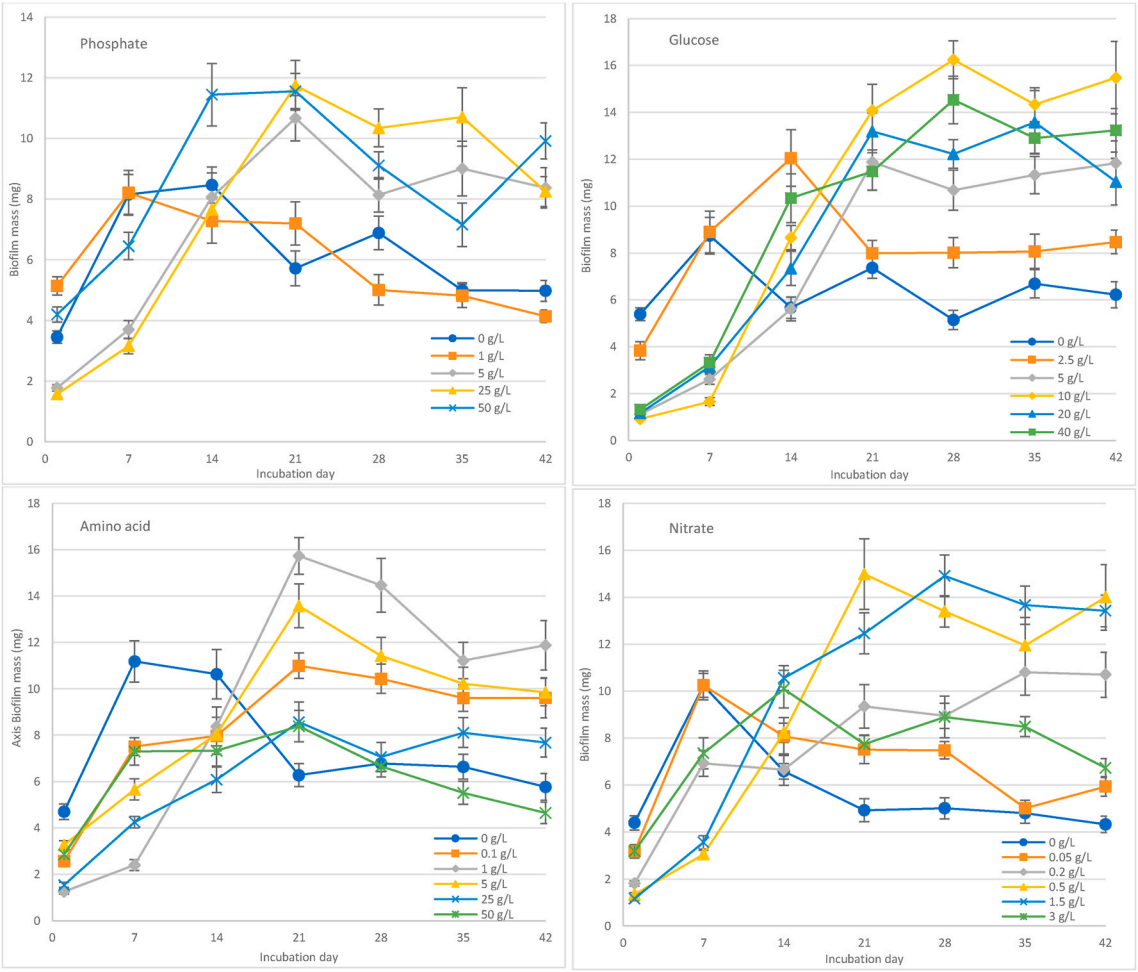

Fig. 3. Effect of concentration of different nutritions on the mass of mixed-species bacterial biofilms on different stages of development. Data are expressed as mean ± standard deviation ($p < 0.05$).

2014). At glucose concentrations higher than the threshold, an osmotic shock occurs which results in a reduction of viable cell densities (Chang et al., 2014). Some authors have stated that the observed increase in the biofilm growth by increasing the glucose content before reaching the threshold, is a result of changes in pH of the medium (Regassa et al., 1992). The results from mass and FTIR analysis of the samples, showed the maximum biofilm mass (16.25 mg) and IR absorbance ratio (0.89) at 10 g L^{-1} of glucose content, which confirmed the highest mixed-species biofilm growth. Moreover, FTIR and mass analysis of the biofilms revealed that at lower concentrations (2.5 g L^{-1}) of glucose in the bioreactor medium, the dispersion stage of the biofilm growth starts earlier (day 14) in comparison with biofilms incubated in a higher content of glucose (day 21 and 28). This observation may be due to the lack of nutrient and shifting the state of the biofilm into stress conditions and as a result, alteration in the composition of the biofilm structure (Paul et al., 2012). The change in the biofilm structure may cause detachment of some parts of the biofilm resulting in the mass and viable cell loss (Petrova and Sauer, 2016).

3.3.3. Amino acid

The effect of amino acid content in the bioreactor medium, on the growth of mixed-species biofilms was evaluated using 3 quantification methods mentioned in section 3.3 and results are presented in Figs. 2–4. According to Fig. 2, increasing the content of amino acid from 0 to 1 gL^{-1} resulted in a 3-log increase in the viable cells. However, further increases of the amino acid to 5, 25 and 50 g L^{-1} showed a 2-, 4- and 6-log decrease in bacterial cells within the 21-days incubated biofilm. This observation was consistent with previous studies. Warraich et al. (2020) reported that higher concentrations of amino acid prevented the attachments of the bacterial cells to the surface and as a result, disrupted the growth of biofilm. Moreover, the reduction in viable cells in higher concentrations of amino acid may be due to reduction in planktonic cell viability (Warraich et al., 2020). Several studies have reported the *anti*-biofilm forming characteristics of amino acid in high concentrations (Kolodkin-Gal et al., 2010; Tong et al., 2014; Yang et al., 2015). However, as shown in Fig. 2, higher concentrations of amino acid (25 and 50 g L^{-1}) had a lower impact on the viable cells in the bioreactor medium in comparison with biofilm. A maximum of 1.5-log decrease was observed when the amino acid content was increased from 1 to 50 g L^{-1} which is lower than the 6-log decrease in viable cells within the biofilm. This observation revealed the fact that although the amino acid prevented the bacterial cells from attaching to the geotextile surface, but did not equally influence the planktonic bacterial growth (Fig. 2).

The analysis of biofilm mass developed by different concentrations of amino acid (Fig. 3) was consistent with the viable cells assay and revealed that amino acid concentrations higher than 1 g L^{-1} resulted in lower biofilm mass. However, Fig. 3 shows that the high concentrations of amino acid are more effective in promoting dispersion of young biofilms (<7days). Previous studies have reported that younger biofilms were more vulnerable to high amino acid content (Vidakovic et al., 2018; Yang et al., 2015). After day 7 of growth, the mass of biofilm incubated in 50 g L^{-1} amino acid content did not increase and experienced a slight constant decrease until day 42. The results of FTIR analysis additionally confirmed that the optimum concentration of amino

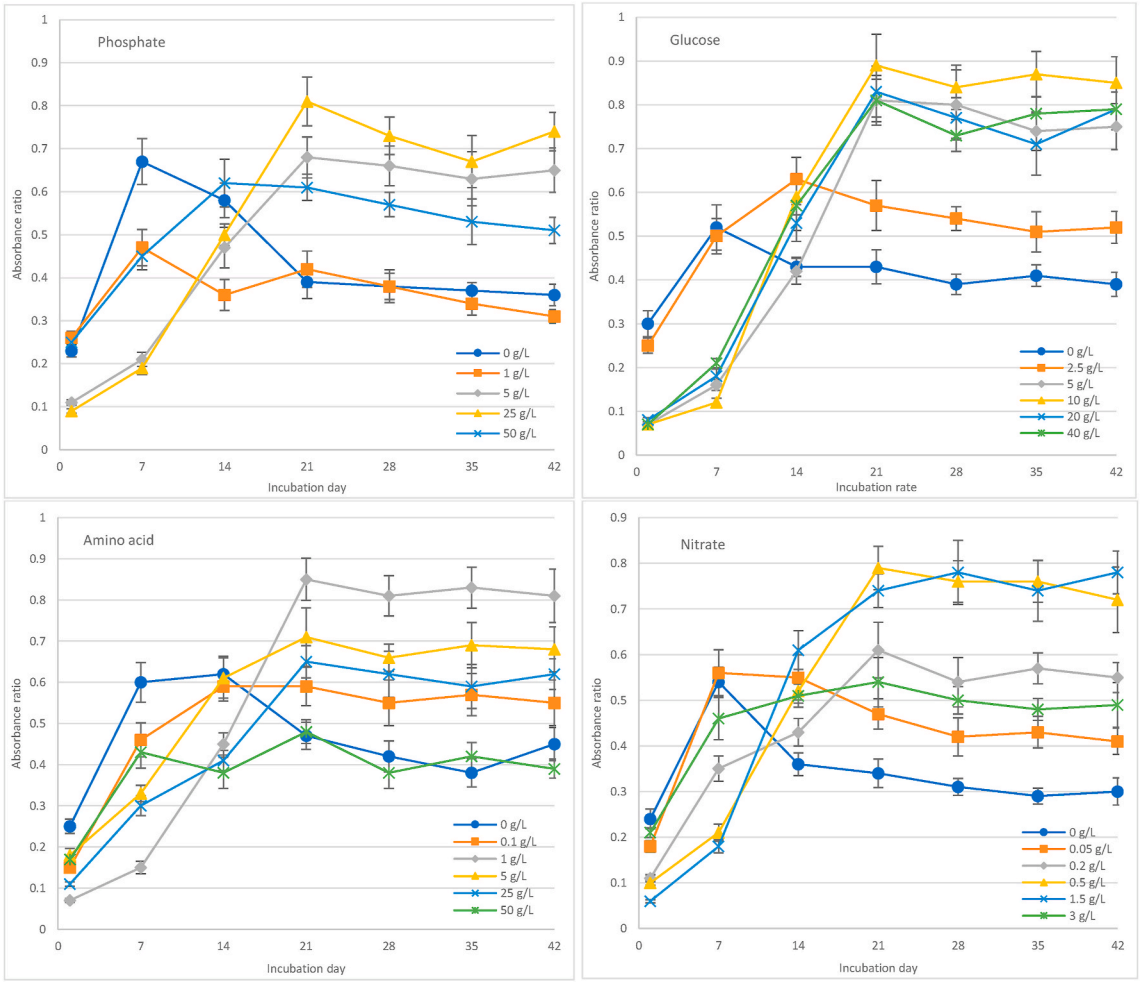

Fig. 4. Effect of concentration of different nutritions on IR absorbance ratio of mixed-species bacterial biofilms on different stages of development. Absorbance ratios are associated with wavelengths of 1078 nm (phosphate groups) and 3384 nm (amine groups). Data are expressed as mean ± standard deviation ($p < 0.05$).

acid for the mixed-species biofilm development on the geotextile in the present study was 1g L^{-1}. The maximum IR absorbance ratio was observed on day 21 of incubation (0.84) and showed a slight decrease and increase cycle on day 28–42 which was due to the dispersion-maturation cycle of the biofilm growth described in section 3.1.

3.3.4. Nitrate

The results of the effect of different concentrations of nitrate on the biofilm growth are shown in Fig. 2. The number of viable cells did not change significantly by increasing the nitrate content of the bioreactor from 0 to 0.2 g L^{-1}. However, the nitrate content of 0.5 and 1.5 g L^{-1} showed a 2-log increase in the number of viable cells on day 21 of biofilm growth. By further increasing the nitrate content to 3 g L^{-1} the number of cells decreased by 0.7-log. This observation revealed that 1.5 g L^{-1} of nitrate content was favourable for the maximum number of viable cells in the biofilm on day 21. The number of viable cells in the bioreactor medium constantly increased with the increase of nitrate content. However, the increase in the number of cells slowed down with 0.5 g L^{-1} to 3 g L^{-1} of nitrate. This observation has been reported in previous studies, that the concentration of nitrate does not affect the biofilm and bacterial growth significantly, in high concentrations as much as it does in low concentrations (Rosier et al., 2020; Martín-Rodríguez et al., 2020; Villemur et al., 2019).

The results of mass analysis of the biofilm (Fig. 3) revealed that the 0.5 and 1.5 g L^{-1} concentrations of nitrate developed denser 21 days incubated biofilms, with a mass of 15 and 12 mg, respectively. The biofilms incubated in different contents of nitrate showed different days to reach the maximum maturation before dispersion phase. The dispersion phase of the biofilm growth occurred on day 21 for biofilms incubated in 0.5 g L^{-1}. However, the dispersion stages started on day 28 for biofilms incubated in 1.5 g L^{-1} of nitrate content. The FTIR absorbance analysis of the biofilms confirmed the highest biofilm growth at 0.5 and 1.5 g L^{-1} of nitrate concentration in the bioreactor with absorbance ratios of 0.79 and 0.78, respectively (Fig. 4). The IR absorbance results also revealed the start of the dispersion stage of the biofilm growth on day 21 and 28 for biofilms incubated in bioreactors with 0.5 and 1.5 g L^{-1} of nitrate concentration, respectively.

3.3.5. Calcium and magnesium

According to Fig. 2, the number of viable cells within the mixed-species biofilms increased constantly with the increase of calcium concentration from 0 to 5 g L^{-1}. However, 10 g L^{-1} concentration of calcium showed a 0.3-log decrease in the number of bacterial cells. A similar observation was reported by previous studies. Dixon et al. (2018) reported an increase in biofilm growth with increasing the calcium ions to 0.5 M. Higher concentrations of calcium were reported to inhibit biofilm growth. Studies have shown the tendency of calcium ions to bind to the negatively charged parts of the EPS and cause disruption and weakening of the biofilm (Somerton et al., 2015; Kara et al., 2008; Sobeck and Higgins, 2002). The number of bacterial cells in the bioreactor medium reached a maximum of 7.1×10^8 CFU mL^{-1} at the calcium concentration

of 0.5 g L^{-1}. With further increase in the calcium concentration, the number of cells decreased. This may have been due to the disruption of regulatory pathways of the bacterial cells resulting in a reduction in the population (Song and Leff, 2006; Michiels et al., 2002). Geesey et al. (2000) reported that calcium ions cause damage to the adhesion molecules of the EPS and reduce the biofilm growth at high concentrations.

The increase in concentration of magnesium ions increased the planktonic growth of the bacterial cell in the bioreactor medium. This increase reached an equilibrium amount of 6.7×10^8 CFU mL^{-1} at 5 and 10 g L^{-1} concentration of magnesium in the bioreactor medium. However, the number of viable cells within the biofilms with concentration of magnesium higher than 0.5 g L^{-1}, decreased significantly (Fig. 4). This observation may be due to the negative influence of the magnesium ions on the production and excretion of EPS proteins, polysaccharides, RNA and eDNA (Dixon et al., 2018; Oknin et al., 2015). Previous studies showed that bacterial species react differently to the magnesium concentration in the medium (Mulcahy and Lewenza, 2011; Gaucheron 2005; Oknin et al., 2015).

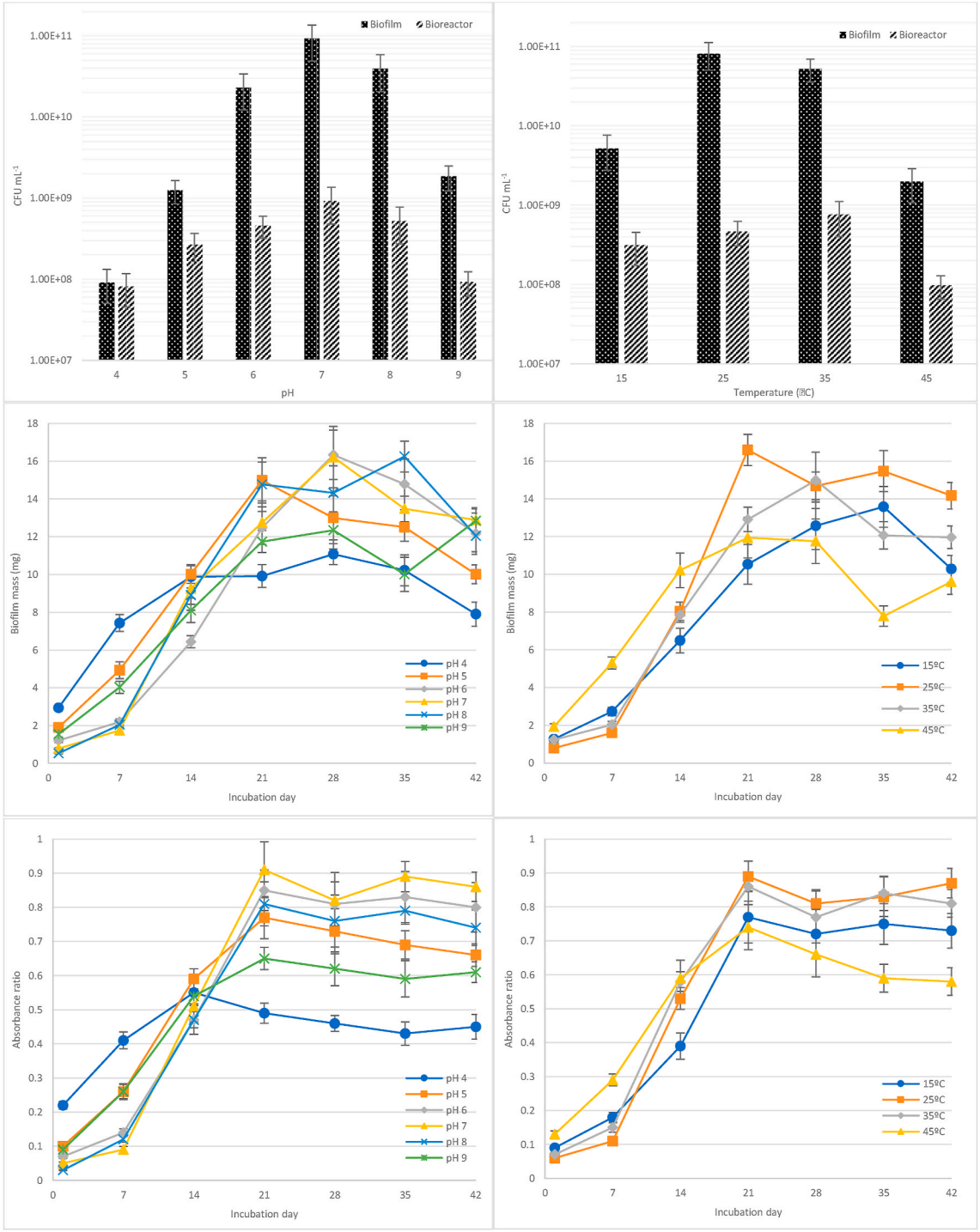

Fig. 5. The effect of temperature and pH on mixed-species biofilm growth quantified using spread plate count, mass analysis and IR absorbance ratios. Values of CFU mL^{-1} are for day 21 of biofilm growth. Absorbance ratios are associated with wavelengths of 1078 nm (phosphate groups) and 3384 nm (amine groups). Data are expressed as mean ± standard deviation ($p < 0.05$).

3.4. Effect environmental conditions on biofilm formation

3.4.1. Effect of pH

The effect of bioreactor medium pH, on the mixed-species bacterial planktonic and biofilm growth, on a nonwoven geotextile, was evaluated in the present study. 3 quantification methods of counting the viable cells, measuring the biofilm mass and analysing the absorbance ratios from the FTIR microscopy of the grown biofilms, were employed to understand the effect of pH on the biofilm growth. The results from spread plates, mass analysis and FTIR microscopy of the mixed-species biofilms incubated in pH 4, 5, 6, 7, 8 and 9 are presented in Fig. 5. According to the number of viable cells, maximum planktonic and biofilm growth was observed at pH 7. By increasing the pH to 9, a 1.8-log decrease in the number of viable cells was detected. Acidic environments showed the same effect on the biofilm growth with a 3-log decrease in bacterial cell number at pH 4. This observation was consistent with previous studies (Papakonstantinou and Efthimiou, 2019; Emanuel et al., 2014; Hoštacká et al., 2010). The reduction in number of bacterial cells in alkaline and acidic pH was due to the fact that pH is critical in maintaining the integrity of cytoplasmic proteins in bacterial cells and the optimum pH for maintaining integrity is 7–7.8 (Cendra et al., 2019; Krulwich et al., 2011; Padan et al., 2005). The same phenomena resulted in reduction of planktonic growth of viable cells in bioreactor medium at pH 4 and 9 with 1.1- and 1-log reduction in the number of cells per 1 mL. However, the effect of pH on the biofilm formation, was more severe than planktonic growth of the bacterial cell as the number of viable cells reduced by 3-log, within the biofilm incubated at pH 4. The results of mass and FTIR analysis (Fig. 5) showed the maximum biofilm mass (16.22 mg) and IR absorbance ratio (0.91) on day 21 of incubation were associated with biofilm grown in bioreactor with pH 7. This observation was consistent with the spread plate technique results and showed that pH 7 is the optimum condition of the growth of biofilm using the mixed-species bacterial culture in the present study.

3.4.2. Effect of temperature

In order to evaluate the effect of temperature on development of mixed-species biofilms, prepared geotextile circles were incubated in bioreactors with controlled temperatures of 15, 25, 35 and 45 °C prior to 3 biofilm quantification assays described in section 3.3. The results from spread plate technique, mass analysis and FTIR microscopy of the mixed-species biofilms incubated at 15, 25, 35 and 45 °C are presented in Fig. 5. According to the results from spread plate technique, the biofilm grown at 25 °C recorded the highest number of viable cells (7.8×10^{10} CFU mL^{-1}). Biofilms incubated at 35 °C contained a 0.2-log lower number of cells. The lowest number of cells was associated to the biofilms grown at 45 °C with 1.9×10^{9} cells on day 21 of incubation. The results from the mass analysis of the biofilm growth, indicated that the biofilm grown in the bioreactor at 25 °C showed the highest mass (15.59 mg). Biofilms incubated at 35, 15 and 45 °C reached their maximum mass of 14.98, 13.18 and 11.61 mg on day 28, 35 and 21, respectively. The FTIR analysis of the biofilm incubated at different temperatures recorded the IR absorbance ratios of 0.77, 0.89, 0.85 and 0.71 for biofilms grown at 15, 25, 35 and 45 °C, respectively. The results from all 3 biofilm quantification assays showed 25 °C as the optimum temperature for the development of the mixed-species biofilm in the present study followed by 35, 15 and 45 °C as less favourable conditions. However, the planktonic growth of the mixed species bacteria culture was reached the maximum number of viable cells for bioreactor with temperature of 35 °C (7.6×10^{8} CFU mL^{-1}). The minimum growth of bacterial cells was associated with bioreactors with temperature of 45 °C with 0.8-log lower number of viable cells in comparison to those incubated at 35 °C. Several studies have reported 25 °C as the optimum temperature for bacterial biofilms (Mizan et al., 2018; Mathlouthi et al., 2018; Herrera et al., 2017; da Silva Meira et al., 2012) and several studies have reported 35 °C as the optimum temperature for the planktonic growth of bacteria (Ricci et al., 2019; Ocampo-Lopez et al., 2015; Mayo and Noike, 1996) which agree with the results from the present study.

3.5. Biosorption studies

3.5.1. Cd(II) removal efficiency and capacity of mixed-species biofilms

In previous sections, the effect of different nutrient concentrations and environmental conditions on mixed-species biofilm development, on a nonwoven geotextile was investigated. In this section, biosorption efficiency and capacity of different stages of biofilm grown in optimized incubation conditions, was evaluated. Geotextile circles were harvested on day 1, 7, 14, 21, 28, 35 and 42 of incubation prior to batch biosorption experiments described in section 2.6. Fig. 6a and b illustrate the Cd(II) removal efficiencies and capacities of different stages of mixed-species biofilm. According to Fig. 6a, the biosorption efficiencies of the biofilm increased as the biofilm became more mature, with the maximum efficiencies occurring on day 35 of incubation. The biosorption efficiencies constantly increased from day 1–21 of incubation. However, on day 28 of growth, a decrease in biosorption efficiencies was observed. On day 35 the Cd(II) removal efficiency of the biofilm showed an increase followed by another phase of decrease on day 42. This observation was consistent with mass and FTIR analysis of the biofilm growth discussed in section 3.3. As discussed earlier, the maturation of the biofilm progressed from day 1 to day 21, resulting in a constant increase in active biosorption sites available on the surface of the biofilm, which equates with higher biosorption efficiencies (Fathollahi et al., 2021). However, between day 21 and 28 the first dispersion stage of the biofilm growth occurred, which led to the first decrease in the removal efficiency. The same pattern occurred between day 35 and 42. The maximum biosorption efficiencies recorded for 0.1, 0.2, 0.5, 1, 2, 5, 10 and 20 mg L^{-1} of Cd(II) were 99, 97, 94, 90, 85, 81, 74 and 69%, respectively (day 35 of incubation).

The results from the Cd(II) biosorption capacities are presented in Fig. 6b. This figure reveals another phenomenon of the biosorption by different stages of biofilm development. According to Fig. 6b, the biosorption efficiency of biofilm incubated for 1 day was the highest amongst all stages of biofilm growth. Biosorption efficiency constantly decreased with the maturation of the biofilm. This observation was due to the monolayer adsorption of the Cd(II) ions by the biofilm. This is because the majority of the active binding sites were available on the surface of the EPS and as the biofilm started to mature and add more internal layers (less active in the biosorption process), the biosorption capacity decreased (Fathollahi et al., 2021b). This finding was not in contrast with the results illustrated in Fig. 6a where the biosorption efficiencies increased with the maturation of the biofilm. In more mature biofilm, the active surface on the EPS layer for the biosorption increased which resulted in higher biosorption efficiencies. However, at the same time, the ratio of biofilm mass actively participating in the biosorption process decreased with biofilm maturation which resulted in lower biosorption capacities (Fathollahi et al., 2020, 2021b). This observation agreed with the mass and FTIR analysis of different stages of biofilm growth described in section 3.3. The maximum mass (Fig. 3) and IR absorbance (Fig. 4) was associated with day 21 of mixed-species biofilm growth which resulted in lowest Cd(II) biosorption capacity. The maximum biosorption capacities recorded for 0.1, 0.2, 0.5, 1, 2, 5, 10 and 20 mg L^{-1} of Cd(II) were 0.76, 1.43, 2.86, 3.82, 5.27, 9.09, 12.74 and 18.19 mg g^{-1}, respectively (day 1 of incubation).

3.5.2. Modelling of Cd(II) biosorption by mixed-species biofilms

Langmuir (1916), Freundlich (1906) and Dubnin Radushkevich (1947) isotherms were used to model the equilibrium the Cd(II) biosorption data, according to the method described by Fathollahi et al. (2020). The linear correlation coefficient (R^2) and isotherm constants were calculated for Langmuir and Freundlich isotherms and are presented in Table 1. The free energy adsorption (E) value was calculated

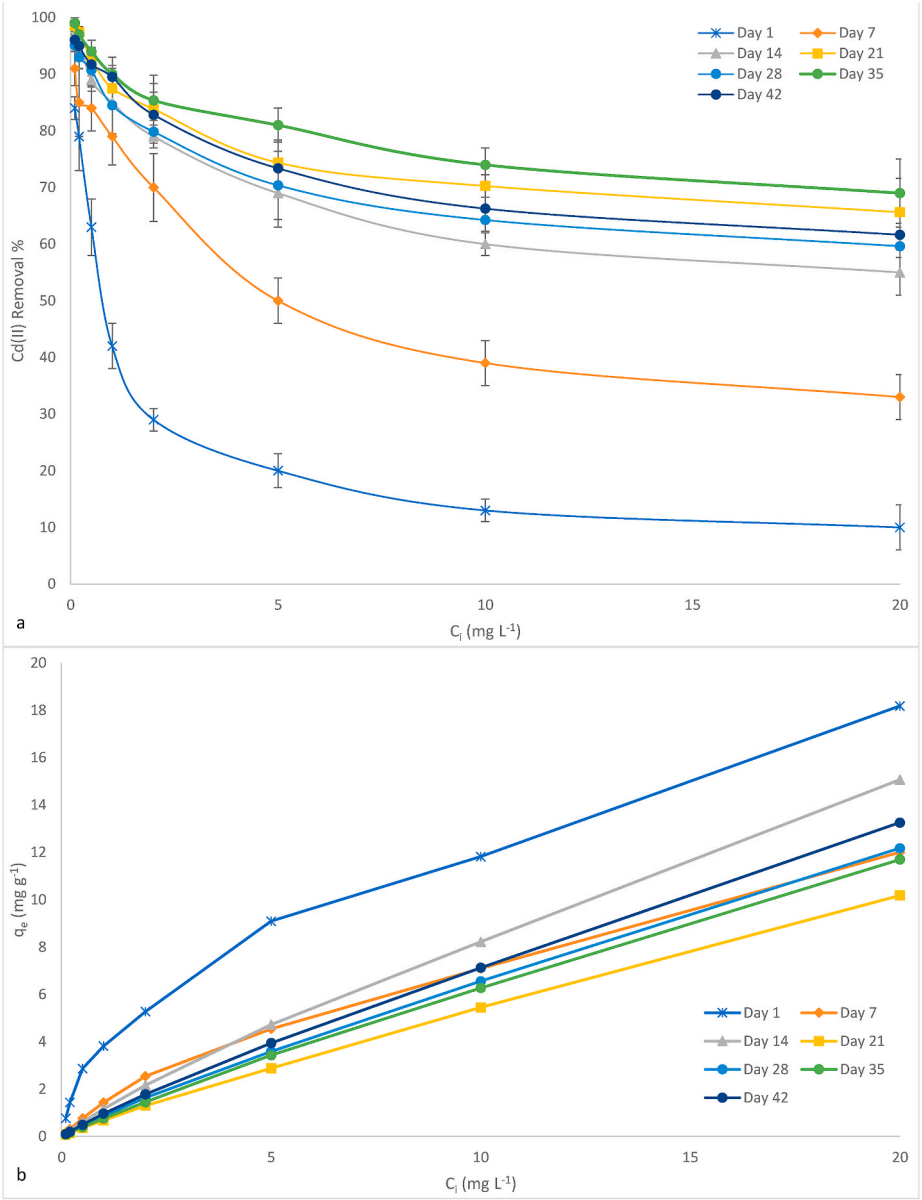

Fig. 6. a) The effect of initial Cd(II) concentration on removal efficiencies of different stages of mixed-species biofilms at pH 5.5, 25 °C and 120 min contact time. b) Modelling of equilibrium Cd(II) biosorption (q_e vs. C_i) for different stages of biofilm growth at pH 5.5 and 25 °C.

Table 1
Constants of Langmuir, Freundlich and D-R isotherms for biosorption of Cd(II) on different stages of mixed-species biofilm development.

	Langmuir Model			Freundlich Model			D-R Model	Isotherm shape
Incubation time	Q_{max} (mg g^{-1})	K_L (L mg^{-1})	R^2	K_F	N	R^2	E (kJ mol^{-1})	
Day 1	18.19	0.21	0.9871	8.1	1.3	0.9091	7.15	L-1
Day 7	12.56	0.16	0.9942	4.5	1.1	0.9195	7.12	L-1
Day 14	15.07	017	0.9937	5.4	1.1	0.9389	7.32	L-1
Day 21	10.17	0.17	0.9963	4.1	1.1	0.9194	7.11	L-1
Day 28	12.68	0.16	0.9997	4.7	1.2	0.9298	7.11	L-1
Day 35	11.71	0.15	0.9983	4.2	1.2	0.9288	7.32	L-1
Day 42	13.25	0.16	0.9924	5.1	1.2	0.9095	7.32	L-1

using the Dubnin Radushkevich (D-R) model in Table 1. The high R^2 values of Langmuir model revealed the monolayer nature of the Cd(II) biosorption by mixed-species biofilms (Chen, 2015). This showed the accuracy of the results from 3.5.1, that more mature biofilms had lower biosorption capacities, due to the inactivity of inner layers of the EPS. This observation was further confirmed, with the results from Freundlich isotherms, with R^2 values lower than the Langmuir model. This indicated that the biosorption did not completely fit the Freundlich model and the Cd(II) removal process was not taking place by multilayer (Ayawei et al., 2017). According to Table 1 and the Langmuir model, the maximum biosorption capacity was 18.19 mg g^{-1} associated with day 1 of incubation and the lowest was 10.17 mg g^{-1} for 21-days grown

biofilm. The modelling results were consistent with batch biosorption results, discussed in section 3.5.1. All phases of biofilm growth had a L1 isotherm shape (Table 1) based on Giles isothermal shape classification (Giles and Smith, 1974). The L1 shape of the isotherms revealed that the active binding sites on the biofilm layer decreased with the increase in the initial concentration of the Cd(II) ions (Hulme and Trevethick, 2010). This was because Cd(II) ions occupied the available binding sites quicker at higher concentrations, resulting in a lower removal efficiency and a L1 isotherm shape (Fig. 6a) (Batoulis et al., 2016).

The E values for all stages of biofilm development are calculated using the D-R model and presented in Table 1. The E (kJ mol^{-1}) parameter is normally used to interpret the dominant biosorption process. In other words, it indicates whether the biosorption process is a chemical ion-exchange or physical adsorption. If $8 < E < 16$ kJ mol^{-1}, the adsorption is classified as a chemical or ion-exchange process, whereas if $E < 8$ kJ mol^{-1}, the biosorption is considered as a physical process (Batool et al., 2018). According to the results, all stages of biofilm had an E value less than 8 kJ mol^{-1} which indicated that the biosorption of Cd(II) by multi-species biofilm was a physical adsorption process.

3.5.3. Control experiments

In order to assess the possible adsorption interference between geotextile fibres and grown mixed-species biofilm, the same batch adsorption experiments were carried out on geotextile circles prepared according to section 2.6.2. The results from control experiments showed no adsorption capacity or efficiency from clean geotextile circles with no biofilm developed on them. This result indicated that the was no interference between geotextile fibres and living biofilms in removal of Cd(II) ions from solution and biosorption efficiencies. Capacities discussed in sections 3.5.1 and 3.5.2 were solely attributed to the mixed-species biofilm layers.

4. Conclusions

The present study evaluated the growth rate of single and mixed cultures of A. meyeri, B. cereus, *E. coli*, P. fluorescens on a nonwoven geotextile. The toxicity of different concentrations of Cd(II) for suspended bacteria and biofilms were evaluated. 7-, 14- and 21-day incubated biofilms of single and mixed-species cultures provided higher protection against Cd(II) ions for bacterial cells. The effect of environmental and nutritional conditions on the bacterial attachment on geotextile surface and the development of the biofilm were determined.

pH 7 was the optimum condition for single and mixed-species biofilm growth. Acidic and alkaline conditions of the growth medium resulted in lower bacterial attachment and growth. Biofilm quantification assays revealed that a temperature between 25 and 35 °C was favourable for the growth of mixed-species bacterial biofilms. However, 45 °C caused severe damage to the attachment and development of the living biofilms. Increasing the concentration of phosphate to 25 g L^{-1} in the bioreactor medium led to higher biofilm growth. Further increases in the phosphate content decreased the bacterial planktonic and biofilm growth. The same trend was observed for concentrations of glucose, amino acid, nitrate, calcium and magnesium with the maximum growth occurring at 10, 1, 1.5, 5 and 0.5 g L^{-1}, respectively.

The mixed species living biofilms developed in the optimum concentration of nutrients and environmental conditions, were harvested in different stages of the growth prior to the batch biosorption experiments. The results of the experiment revealed that the maximum biosorption efficiency (99%) occurred at day 35 of biofilm growth for 0.1 mg L^{-1} of Cd(II). The lowest biosorption efficiency (84%) for 0.1 mgL^{-1} of Cd(II) was observed on day 1 of incubation. However, 1-day incubated mixed-species biofilm had the highest biosorption capacity (18.19 mg g^{-1}) due to the optimum EPS surface to mass ratio. Langmuir, Freundlich and Dubnin Radushkevich modelling of the biosorption data, revealed that the Cd(II) removal by the mixed species living biofilms was a physical adsorption process. Monolayers were responsible for Cd(II) removal and the L1 shape of the isotherms revealed the high affinity of the living biofilm for the Cd(II) ions at low concentrations.

Funding

This project has received funding from the European Union's Horizon 2020 research and innovation program under the Marie Sklodowska-Curie grant No 765057, project name SAFERUP!

Credit author statement

Alireza Fathollahi: Conceptualization, Methodology, Validation, Formal analysis, Investigation, Resources, Writing – original draft, Writing – review & editing. Stephen J Coupe: Conceptualization, Methodology, Validation, Investigation, Resources, Writing – review & editing, Supervision, Project administration.

Declaration of competing interest

The authors declare that they have no known competing financial interests or personal relationships that could have appeared to influence the work reported in this paper.

References

Abebe, G.M., 2020. The role of bacterial biofilm in antibiotic resistance and food contamination. Internet J. Microbiol. https://doi.org/10.1155/2020/1705814.
Adewuyi, A., 2020. Chemically Modified Biosorbents and Their Role in the Removal of Emerging Pharmaceuticalwaste in the Water System. Water, Switzerland. https://doi.org/10.3390/W12061551.
Amari, T., Ghnaya, T., Abdelly, C., 2017. Nickel, cadmium and lead phytotoxicity and potential of halophytic plants in heavy metal extraction. South Afr. J. Bot. https://doi.org/10.1016/j.sajb.2017.03.011.
Ayawei, N., Ebelegi, A.N., Wankasi, D., 2017. Modelling and interpretation of adsorption isotherms. J. Chem. https://doi.org/10.1155/2017/3039817.
Baquero, F., Negri, M.C., 1997. Selective compartments for resistant microorganisms in antibiotic gradients. Bioessays. https://doi.org/10.1002/bies.950190814.
Bashir, I., Lone, F.A., Bhat, R.A., Mir, S.A., Dar, Z.A., Dar, S.A., 2020. Concerns and threats of contamination on aquatic ecosystems. In: Bioremediation and Biotechnology: Sustainable Approaches to Pollution Degradation. https://doi.org/10.1007/978-3-030-35691-0_1.
Batool, F., Akbar, J., Iqbal, S., Noreen, S., Bukhari, S.N.A., 2018. Study of isothermal, kinetic, and thermodynamic parameters for adsorption of cadmium: an overview of linear and nonlinear approach and error analysis. Bioinorgan. Chem. Appl. https://doi.org/10.1155/2018/3463724.
Batoulis, H., Schmidt, T.H., Weber, P., Schloetel, J.G., Kandt, C., Lang, T., 2016. Concentration dependent ion-protein interaction patterns underlying protein oligomerization behaviours. Sci. Rep. https://doi.org/10.1038/srep24131.
Becouze-Lareure, C., Dembélé, A., Coquery, M., Cren-Olivé, C., Barillon, B., Bertrand-Krajewski, J.L., 2016. Source Characterisation and Loads of Metals and Pesticides in Urban Wet Weather Discharges. Urban Water J. https://doi.org/10.1080/1573062X.2015.1011670.
Beloin, C., Roux, A., Ghigo, J.M., 2008. Escherichia coli biofilms. Curr. Top. Microbiol. Immunol. https://doi.org/10.1007/978-3-540-75418-3_12.
Bibby, S.R.S., Urban, J.P.G., 2004. Effect of nutrient deprivation on the viability of intervertebral disc cells. Eur. Spine J. https://doi.org/10.1007/s00586-003-0616-x.
Brinza, L., Dring, M.J., Gavrilescu, M., 2007. Marine micro and macro algal species as biosorbents for heavy metals. Environ. Eng. Manag. J. https://doi.org/10.30638/eemj.2007.029.
Brocker, C., Thompson, D.C., Vasiliou, V., 2012. The role of hyperosmotic stress in inflammation and disease. Biomol. Concepts. https://doi.org/10.1515/bmc-2012-0001.
Calicioglu, O., Shreve, M.J., Richard, T.L., Brennan, R.A., 2018. Effect of pH and temperature on microbial community structure and carboxylic acid yield during the acidogenic digestion of duckweed. Biotechnol. Biofuels. https://doi.org/10.1186/s13068-018-1278-6.
Cendra, M., del, M., Blanco-Cabra, N., Pedraz, L., Torrents, E., 2019. Optimal environmental and culture conditions allow the in vitro coexistence of Pseudomonas aeruginosa and Staphylococcus aureus in stable biofilms. Sci. Rep. https://doi.org/10.1038/s41598-019-52726-0.
Chang, J., Coleman, S., Lee, Y.E., Schellenberg-Beaver, T., 2014. Differential effects of sucrose or NaCl osmotic shock on βgalactosidase activity in Escherichia coli BW25993 is dependent on normalization method by total viable count or total protein content. J. Exp. Microbiol. Immunol. 18, 54–59.
Charlesworth, S., Harker, E., Rickard, S., 2003. A Review of Sustainable Drainage Systems (SuDS) (Geography).

Chen, X., 2015. Modeling of experimental adsorption isotherm data. Inf. https://doi.org/10.3390/info6010014.
da Silva Meira, Q.G., de Medeiros Barbosa, I., Alves Aguiar Athayde, A.J., de Siqueira-Júnior, J.P., de Souza, E.L., 2012. Influence of temperature and surface kind on biofilm formation by Staphylococcus aureus from food-contact surfaces and sensitivity to sanitizers. Food Contr. https://doi.org/10.1016/j.foodcont.2011.11.030.
Decho, A.W., Gutierrez, T., 2017. Microbial extracellular polymeric substances (EPSs) in ocean systems. Front. Microbiol. https://doi.org/10.3389/fmicb.2017.00922.
Di Martino, P., 2018. Extracellular polymeric substances, a key element in understanding biofilm phenotype. AIMS Microbiol. https://doi.org/10.3934/microbiol.2018.2.274.
Dixon, M.J.L., Flint, S.H., Palmer, J.S., Love, R., Chabas, C., Beuger, A.L., 2018. The effect of calcium on biofilm formation in dairy wastewater. Water Pract. Technol. https://doi.org/10.2166/wpt.2018.050.
Doelman, P., Haanstra, L., 1984. Short-term and long-term effects of cadmium, chromium, copper, nickel, lead and zinc on soil microbial respiration in relation to abiotic soil factors. Plant Soil. https://doi.org/10.1007/BF02184325.
Donlan, R.M., 2002. Biofilms: microbial life on surfaces. Emerg. Infect. Dis. https://doi.org/10.3201/eid0809.020063.
Dubinin, M.M., Radushkevich, L.V., 1947. Equation of the characteristic curve of activated charcoal. Proc. Acad. Sci. USSR Phys. Chem. Sect.
Elias, S., Banin, E., 2012. Multi-species biofilms: living with friendly neighbors. FEMS Microbiol. https://doi.org/10.1111/j.1574-6976.2012.00325.x.
Emanuel, V., Adrian, V., Diana, P., 2010. Microbial biofilm formation under the influence of various physical-chemical factors. Biotechnol. Biotechnol. Equip. https://doi.org/10.2478/V10133-010-0056-9.
Enaime, G., Baçaoui, A., Yaacoubi, A., Lübken, M., 2020. Biochar for wastewater treatment-conversion technologies and applications. Appl. Sci. https://doi.org/10.3390/app10103492.
Fan, Y., Huang, X., Chen, J., Han, B., 2020. formation of a mixed-species biofilm is a survival strategy for unculturable lactic acid bacteria and Saccharomyces cerevisiae in daqu, a Chinese traditional fermentation starter. Front. Microbiol. https://doi.org/10.3389/fmicb.2020.00138.
Fathollahi, A., Coupe, S.J., 2021. Life cycle assessment and life cycle costing of road drainage systems for sustainability evaluation: quantifying the contribution of different life cycle phases. Sci. Total Environ. 776 https://doi.org/10.1016/j.scitotenv.2021.145937.
Fathollahi, A., Coupe, S.J., El-Sheikh, A.H., Sañudo-Fontaneda, L.A., 2020. The biosorption of mercury by permeable pavement biofilms in stormwater attenuation. Sci. Total Environ. https://doi.org/10.1016/j.scitotenv.2020.140411.
Fathollahi, A., Khasteganan, N., Coupe, S.J., Newman, A.P., 2021a. A meta-analysis of metal biosorption by suspended bacteria from three phyla. Chemosphere. https://doi.org/10.1016/j.chemosphere.2020.129290.
Fathollahi, A., Coupe, S.J., El-Sheikh, A.H., Nnadi, E.O., 2021b. Cu(II) biosorption by living biofilms: isothermal, chemical, physical and biological evaluation. J. Environ. Manag. https://doi.org/10.1016/j.jenvman.2021.111950.
Freundlich, H.M.F., 1906. Over the adsorption in solution. J. Phys. Chem.
Gasperi, J., Sebastian, C., Ruban, V., Delamain, M., Percot, S., Wiest, L., Mirande, C., Caupos, E., Demare, D., Kessoo, M.D.K., Saad, M., Schwartz, J.J., Dubois, P., Fratta, C., Wolff, H., Moilleron, R., Chebbo, G., Cren, C., Millet, M., Barraud, S., Gromaire, M.C., 2014. Micropollutants in urban stormwater: occurrence, concentrations, and atmospheric contributions for a wide range of contaminants in three French catchments. Environ. Sci. Pollut. Res. https://doi.org/10.1007/s11356-013-2396-0.
Geesey, G.G., Wigglesworth-Cooksey, B., Cooksey, K.E., 2000. Influence of calcium and other cations on surface adhesion of bacteria and diatoms: a review. In: Biofouling. https://doi.org/10.1080/08927010009386310.
Giles, C.H., Smith, D., Huitson, A., 1974. A general treatment and classification of the solute adsorption isotherm. I. Theoretical. J. Colloid Interface Sci. https://doi.org/10.1016/0021-9797(74)90252-5.
Gulati, M., Nobile, C.J., 2016. Candida albicans biofilms: development, regulation, and molecular mechanisms. Microb. Infect. https://doi.org/10.1016/j.micinf.2016.01.002.
Gupta, P., Diwan, B., 2017. Bacterial Exopolysaccharide mediated heavy metal removal: a Review on biosynthesis, mechanism and remediation strategies. Biotechnol. Rep. https://doi.org/10.1016/j.btre.2016.12.006.
Gwenzi, W., Nyamadzawo, G., 2014. Hydrological impacts of urbanization and urban roof water harvesting in water-limited catchments: a review. Environ. Process. https://doi.org/10.1007/s40710-014-0037-3.
Haney, E.F., Trimble, M.J., Cheng, J.T., Vallé, Q., Hancock, R.E.W., 2018. Critical assessment of methods to quantify biofilm growth and evaluate antibiofilm activity of host defence peptides. Biomolecules. https://doi.org/10.3390/biom8020029.
Harmsen, M., Yang, L., Pamp, S.J., Tolker-Nielsen, T., 2010. An update on Pseudomonas aeruginosa biofilm formation, tolerance, and dispersal. FEMS Immunol. Med. Microbiol. https://doi.org/10.1111/j.1574-695X.2010.00690.x.
Hassan, Sahar W., 2011. Biosorption of cadmium from aqueous solutions using A local fungus Aspergillus cristatus (glaucus group). African J. Biotechnol. https://doi.org/10.5897/ajb11.3140.
Herrera, J.J.R., Cabo, M.L., González, A., Pazos, I., Pastoriza, L., 2007. Adhesion and detachment kinetics of several strains of Staphylococcus aureus subsp. aureus under three different experimental conditions. Food Microbiol. https://doi.org/10.1016/j.fm.2007.01.001.
Hoštacká, A., Čižnár, I., Štefkovičová, M., 2010. Temperature and pH affect the production of bacterial biofilm. Folia Microbiol. https://doi.org/10.1007/s12223-010-0012-y (Praha).
Hulme, E.C., Trevethick, M.A., 2010. Ligand binding assays at equilibrium: Validation and interpretation. Br. J. Pharmacol. https://doi.org/10.1111/j.1476-5381.2009.00604.x.
Ismail, I., Sulaymon, Abbas Hamid, Hussein, Abbas Salman, Abbas, Salman H., Ismail, I. M., Mostafa, T.M., Sulaymon, Abbas H., 2014. Bisorption of heavy metals: a review biosorption of heavy metals: a review. J. Chem. Sci. Technol.
Jaishankar, M., Tseten, T., Anbalagan, N., Mathew, B.B., Beeregowda, K.N., 2014. Toxicity, mechanism and health effects of some heavy metals. Interdiscipl. Toxicol. https://doi.org/10.2478/intox-2014-0009.
Kaplan, J.B., 2010. Biofilm dispersal: mechanisms, clinical implications, and potential therapeutic uses. J. Dent. Res. https://doi.org/10.1177/0022034509359403.
Kara, F., Gurakan, G.C., Sanin, F.D., 2008. Monovalent cations and their influence on activated sludge floc chemistry, structure, and physical characteristics. Biotechnol. Bioeng. https://doi.org/10.1002/bit.21755.
Karygianni, L., Ren, Z., Koo, H., Thurnheer, T., 2020. Biofilm matrixome: extracellular components in structured microbial communities. Trends Microbiol. https://doi.org/10.1016/j.tim.2020.03.016.
Koechler, S., Farasin, J., Cleiss-Arnold, J., Arsène-Ploetze, F., 2015. Toxic metal resistance in biofilms: diversity of microbial responses and their evolution. Res. Microbiol. https://doi.org/10.1016/j.resmic.2015.03.008.
Kolodkin-Gal, I., Romero, D., Cao, S., Clardy, J., Kolter, R., Losick, R., 2010. D-Amino acids trigger biofilm disassembly. Science 80–. https://doi.org/10.1126/science.1188628.
Kostakioti, M., Hadjifrangiskou, M., Hultgren, S.J., 2013. Bacterial biofilms: development, dispersal, and therapeutic strategies in the dawn of the postantibiotic era. Cold Spring Harb. Perspect. Med. https://doi.org/10.1101/cshperspect.a010306.
Krulwich, T.A., Sachs, G., Padan, E., 2011. Molecular aspects of bacterial pH sensing and homeostasis. Nat. Rev. Microbiol. https://doi.org/10.1038/nrmicro2549.
Langmuir, I., 1917. The constitution and fundamental properties of solids and liquids. II. Liquids. J. Am. Chem. Soc. https://doi.org/10.1021/ja02254a006.
Mamisahebei, S., Jahed Khaniki, G.R., Torabian, A., Nasseri, S., Naddafi, K., 2007. Removal of arsenic from an aqueous solution by pretreated waste tea fungal biomass. Iran. J. Environ. Heal. Sci. Eng.
Martín-Rodríguez, A.J., Rhen, M., Melican, K., Richter-Dahlfors, A., 2020. Nitrate metabolism modulates biosynthesis of biofilm components in uropathogenic Escherichia coli and acts as a fitness factor during experimental urinary tract infection. Front. Microbiol. https://doi.org/10.3389/fmicb.2020.00026.
Martínez-Juárez, V.M., Cárdenas-González, J.F., Torre-Bouscoulet, M.E., Acosta-Rodríguez, I., 2012. Biosorption of mercury (II) from aqueous solutions onto fungal biomass. Bioinorgan. Chem. Appl. https://doi.org/10.1155/2012/156190.
Mathlouthi, A., Pennacchietti, E., De Biase, D., 2018. Effect of temperature, pH and plasmids on in vitro biofilm formation in Escherichia coli. Acta Naturae. https://doi.org/10.32607/20758251-2018-10-4-129-132.
Mayo, A.W., Noike, T., 1996. Effects of temperature and pH on the growth of heterotrophic bacteria in waste stabilization ponds. Water Res. https://doi.org/10.1016/0043-1354(95)00150-6.
McGrane, S.J., 2016. Impacts of urbanisation on hydrological and water quality dynamics, and urban water management: a review. Hydrol. Sci. J. https://doi.org/10.1080/02626667.2015.1128084.
McGrath, S.P., 1999. Adverse effects of cadmium on soil microflora and fauna. Cadmium in Soils and Plants. https://doi.org/10.1007/978-94-011-4473-5_8.
Michalak, I., Chojnacka, K., Witek-Krowiak, A., 2013. State of the art for the biosorption process - a review. Appl. Biochem. Biotechnol. https://doi.org/10.1007/s12010-013-0269-0.
Michiels, J., Xi, C., Verhaert, J., Vanderleyden, J., 2002. The functions of Ca2+ in bacteria: a role for EF-hand proteins? Trends Microbiol. https://doi.org/10.1016/S0966-842X(01)02284-3.
Mizan, M.F.R., Jahid, I.K., Park, S.Y., Silva, J.L., Kim, T.J., Myoung, J., Ha, S.D., 2018. Effects of temperature on biofilm formation and quorum sensing of aeromonas hydrophila. Ital. J. Food Sci. https://doi.org/10.14674/IJFS-1004.
Mulcahy, H., Lewenza, S., 2011. Magnesium limitation is an environmental trigger of the pseudomonas aeruginosa biofilm lifestyle. PloS One. https://doi.org/10.1371/journal.pone.0023307.
Müller, A., Österlund, H., Marsalek, J., Viklander, M., 2020. The pollution conveyed by urban runoff: a review of sources. Sci. Total Environ. https://doi.org/10.1016/j.scitotenv.2019.136125.
Ocampo-López, C., Colorado-Arias, S., Ramírez-Carmona, M., 2015. Modeling of microbial growth and ammonia consumption at different temperatures in the production of a polyhydroxyalkanoate (PHA) biopolymer. J. Appl. Res. Technol. https://doi.org/10.1016/j.jart.2015.10.001.
Oknin, H., Steinberg, D., Shemesh, M., 2015. Magnesium ions mitigate biofilm formation of Bacillus species via downregulation of matrix genes expression. Front. Microbiol. https://doi.org/10.3389/fmicb.2015.00907.
Padan, E., Bibi, E., Ito, M., Krulwich, T.A., 2005. Alkaline pH homeostasis in bacteria: new insights. Biochim. Biophys. Acta Biomembr. https://doi.org/10.1016/j.bbamem.2005.09.010.
Papakonstantinou, K., Efthimiou, G., 2019. Investigating the effect of alkaline stress on biofilm formation by Salmonella enteritidis. Access Microbiol. https://doi.org/10.1099/acmi.ac2019.po0453.
Paul, E., Ochoa, J.C., Pechaud, Y., Liu, Y., Liné, A., 2012. Effect of shear stress and growth conditions on detachment and physical properties of biofilms. Water Res. https://doi.org/10.1016/j.watres.2012.07.029.
Petrova, O.E., Sauer, K., 2016. Escaping the biofilm in more than one way: desorption, detachment or dispersion. Curr. Opin. Microbiol. https://doi.org/10.1016/j.mib.2016.01.004.

Pugazhenthiran, N., Anandan, S., Ashokkumar, M., 2016. Removal of heavy metal from wastewater #26. Handbook of Ultrasonics and Sonochemistry. https://doi.org/10.1007/978-981-287-278-4_58.

Ramsenthil, R., Meyyappan, R., 2010. Single and multi-component biosorption of copper and zinc ions using microalgal resin. Int. J. Environ. Sustain Dev. https://doi.org/10.7763/ijesd.2010.v1.58.

Reezal, A., Mcneil, B., Anderson, J.G., 1998. Effect of low-osmolality nutrient media on growth and culturability of Campylobacter species. Appl. Environ. Microbiol. https://doi.org/10.1128/aem.64.12.4643-4649.1998.

Regassa, L.B., Novick, R.P., Betley, M.J., 1992. Glucose and nonmaintained pH decrease expression of the accessory gene regulator (agr) in Staphylococcus aureus. Infect. Immun. https://doi.org/10.1128/iai.60.8.3381-3388.1992.

Ricci, S., Pinette, M.G., Wax, J.R., Craig, W., Forrest, L., Dragoni, C., 2020. The effect of temperature on bacterial growth in the presence of nonsterile ultrasound coupling gel. Am. J. Obstet. Gynecol. https://doi.org/10.1016/j.ajog.2019.10.001.

Rosier, B.T., Buetas, E., Moya-Gonzalvez, E.M., Artacho, A., Mira, A., 2020. Nitrate as a potential prebiotic for the oral microbiome. Sci. Rep. https://doi.org/10.1038/s41598-020-69931-x.

Saini, R., Saini, S., Sharma, S., 2011. Biofilm: a dental microbial infection. J. Nat. Sci. Biol. Med. https://doi.org/10.4103/0976-9668.82317.

Sakson, G., Brzezinska, A., Zawilski, M., 2018. Emission of heavy metals from an urban catchment into receiving water and possibility of its limitation on the example of Lodz city. Environ. Monit. Assess. https://doi.org/10.1007/s10661-018-6648-9.

Salgar-Chaparro, S.J., Lepkova, K., Pojtanabuntoeng, T., Darwin, A., Machuca, L.L., 2020. Nutrient level determines biofilm characteristics and subsequent impact on microbial corrosion and biocide effectiveness. Appl. Environ. Microbiol. https://doi.org/10.1128/AEM.02885-19.

Selbig, W.R., Bannerman, R., Corsi, S.R., 2013. From streets to streams: assessing the toxicity potential of urban sediment by particle size. Sci. Total Environ. https://doi.org/10.1016/j.scitotenv.2012.11.094.

Sheikha, D., Ashour, I., Abu Al-Rub, F.A., 2008. Biosorption of zinc on immobilized green algae: equilibrium and dynamics studies. J. Eng. Res. https://doi.org/10.24200/tjer.vol5iss1pp20-29 [TJER].

Sobeck, D.C., Higgins, M.J., 2002. Examination of three theories for mechanisms of cation-induced bioflocculation. Water Res. https://doi.org/10.1016/S0043-1354(01)00254-8.

Somerton, B., Lindsay, D., Palmer, J., Brooks, J., Flint, S., 2015. Changes in sodium, calcium, and magnesium ion concentrations that inhibit Geobacillus biofilms have no effect on Anoxybacillus flavithermus biofilms. Appl. Environ. Microbiol. https://doi.org/10.1128/AEM.01037-15.

Song, B., Leff, L.G., 2006. Influence of magnesium ions on biofilm formation by Pseudomonas fluorescens. Microbiol. Res. https://doi.org/10.1016/j.micres.2006.01.004.

Šovljanski, O., Tomić, A., Pezo, L., Markov, S., 2020. Temperature and pH growth profile prediction of newly isolated bacterial strains from alkaline soils. J. Sci. Food Agric. https://doi.org/10.1002/jsfa.10124.

Stewart, P.S., 2003. Diffusion in biofilms. J. Bacteriol. https://doi.org/10.1128/JB.185.5.1485-1491.2003.

Tchounwou, P.B., Yedjou, C.G., Patlolla, A.K., Sutton, D.J., 2012. Heavy Metal Toxicity and the Environment. EXS. https://doi.org/10.1007/978-3-7643-8340-4_6.

Tong, Z., Zhang, L., Ling, J., Jian, Y., Huang, L., Deng, D., 2014. An in vitro study on the effect of free amino acids alone or in combination with nisin on biofilms as well as on planktonic bacteria of Streptococcus mutans. PloS One. https://doi.org/10.1371/journal.pone.0099513.

Uribe-Lorío, L., Brenes-Guillén, L., Hernández-Ascencio, W., Mora-Amador, R., González, G., Ramírez-Umaña, C.J., Díez, B., Pedrós-Alió, C., 2019. The influence of temperature and pH on bacterial community composition of microbial mats in hot springs from Costa Rica. Microbiologyopen. https://doi.org/10.1002/mbo3.893.

Vidakovic, L., Singh, P.K., Hartmann, R., Nadell, C.D., Drescher, K., 2017. Dynamic biofilm architecture confers individual and collective mechanisms of viral protection. Nat. Microbiol. https://doi.org/10.1038/s41564-017-0050-1.

Villemur, R., Payette, G., Geoffroy, V., Mauffrey, F., Martineau, C., 2019. Impact of NaCl, nitrate and temperature on the microbial community of a methanol-fed, denitrifying marine biofilm. bioRxiv. https://doi.org/10.1101/607028.

Vincent, J.M., 1970. A Manual for the Practical Study of Root-Nodule Bacteria. I.B.P. Handbook. Blackwell Sci. Publ., Oxford, UK, 1970.

Waldrop, R., McLaren, A., Calara, F., McLemore, R., 2014. Biofilm growth has a threshold response to glucose in vitro. Clin. Orthop. Relat. Res. https://doi.org/10.1007/s11999-014-3538-5.

Walsh, C.J., Fletcher, T.D., Burns, M.J., 2012. Urban stormwater runoff: a new class of environmental flow problem. PloS One. https://doi.org/10.1371/journal.pone.0045814.

Wang, J., Zhao, Y., Yang, L., Tu, N., Xi, G., Fang, X., 2017. Removal of Heavy Metals from Urban Stormwater Runoff Using Bioretention Media Mix. Water (Switzerland). https://doi.org/10.3390/w9110854.

Warraich, A.A., Mohammed, A.R., Perrie, Y., Hussain, M., Gibson, H., Rahman, A., 2020. Evaluation of anti-biofilm activity of acidic amino acids and synergy with ciprofloxacin on Staphylococcus aureus biofilms. Sci. Rep. https://doi.org/10.1038/s41598-020-66082-x.

Yang, H., Wang, M., Yu, J., Wei, H., 2015. Aspartate inhibits Staphylococcus aureus biofilm formation. FEMS Microbiol. Lett. https://doi.org/10.1093/femsle/fnv025.

Yin, W., Wang, Y., Liu, L., He, J., 2019. Biofilms: the microbial “protective clothing” in extreme environments. Int. J. Mol. Sci. https://doi.org/10.3390/ijms20143423.

Zgheib, S., Moilleron, R., Chebbo, G., 2012. Priority pollutants in urban stormwater: Part 1 - case of separate storm sewers. Water Res. https://doi.org/10.1016/j.watres.2011.12.012.